Extraction of Atrial Activity from the ECG by Spectrally Constrained ICA Based on Kurtosis Sign

Ronald Phlypo[1,2,⋆], Vicente Zarzoso[1], Pierre Comon[1], Yves D'Asseler[2], and Ignace Lemahieu[2]

[1] Laboratoire I3S, CNRS/UNSA Les Algorithmes - Euclide-B, BP 121, 2000 Route des Lucioles, 06903 Sophia Antipolis Cedex, France
{phlypo,zarzoso,pcomon}@i3s.unice.fr
[2] MEDISIP-IBBT, ELIS/UGent, IBiTech - Campus Heymans, De Pintelaan 185, B-9000 Ghent, Belgium
{ronald.phlypo,yves.dasseler,ignace.lemahieu}@ugent.be

Abstract. This paper deals with the problem of estimating atrial activity during atrial fibrillation periods in the electrocardiogram (ECG). Since the signal of interest differs in kurtosis sign from the dominant sources in the ECG, we propose an independent component analysis method for source extraction based on the different kurtosis sign and extend it with a constraint of spectral concentration in the 3-12Hz frequency band. Results show that we are able to estimate the atrial fibrillation with a single algorithm having low computational complexity ($\mathcal{O}$(7n-7)T).

1 Introduction

This paper describes a method to recover narrow band independent signals from a linear mixture model where high impulsive (high kurtosis) signals are the main source of interference. This set-up is a commonly encountered problem in biomedical signal analysis, e.g. when considering spectral bands of activity in electroencephalographic recordings or atrial fibrillation (AF) signals in the electro cardiogram (ECG) where the main sources of interference are respectively the ocular activity and the QRS(-T) complex.

The focus here is on the recovery of atrial activity during AF from an ECG recording, whatever the conditions of noise or interference from other physiological signals (e.g. QRS complex). Since we consider narrow band spectra in a volume conductor, a linear approximation of the electromagnetic Maxwell equations is valid and hence we may suppose that a general linear mixing model holds. This mixture model translates the measured potentials at the chest or body surface into bio-electrical source signals (generally specified by their currents) and *vice versa*. If we consider the mixing-demixing model, all relations exhibit the

⋆ R. Phlypo would like to thank H. Rix and V. Zarzoso for their kind hospitality at the laboratories of I3S.

M.E. Davies et al. (Eds.): ICA 2007, LNCS 4666, pp. 641–648, 2007.

characteristics of a linear model and thus we can rewrite our system of measurements $\boldsymbol{y}$ into an equivalent set of potentials $\boldsymbol{x}$, where each x_i is associated with a column of $\boldsymbol{A}, \boldsymbol{a}_i$. The latter represent the mappings of the sources on the measurement surface (known as source topographies). Or, in matrix notation:

$$\boldsymbol{y}(t) = \boldsymbol{A}\boldsymbol{x}(t) + \eta(t), \tag{1}$$

which explains the relations between the measurements $\boldsymbol{y} \in \mathbb{R}^{m\times 1}$, the mixing matrix $\boldsymbol{A} \in \mathbb{R}^{m\times n}$, the sources $\boldsymbol{x} \in \mathbb{R}^{n\times 1}$ and the noise $\eta \in \mathbb{R}^{m\times 1}$.

The measurements and the sources can be seen as realisations of random variables. Therefore we will drop the time index in the subsequent work to improve readability. For the biomedical case we might assume that these sources are quasi statistically independent. In the case of atrial fibrillation, we can restrict the AF source characteristics even further by imposing the extra constraint that the AF signal should have a narrow band spectrum, thus having platokurtic statistics. This is in contrast to the QRS(-T) complex - the main masking source - which is highly leptokurtic (see e.g. [1]). In the rest of this paper we will develop this idea further, sketching a framework in which we can extract the independent AF source based on the difference in kurtosis sign and under the constraint of narrow band source spectra. The solution is given as the ensemble of subsequent algebraic solutions to the pairwise separation problem, subjected to a conditional update. This guarantees a robust algorithm, with only few parameters to estimate and omitting the need for exhaustive search algorithms.

2 Methods

2.1 The Kurtic Difference as an Object Function to ICA

ICA. The solution to the ICA problem has been proposed by different authors, using different contrast functions. Despite the diversity at the basis of the algorithms, the solution space is almost always given by components whose higher order cross cumulants vanish [2,3], which in its turn is equivalent to a reduction of the mutual information between the components [4,5]. Solutions have been proposed to solve the problem by deflation approaches [6] - estimating source by source - or to interact on the whole subset at once. The deflation approach offers the ability to solve for independence in a component-by-component way, sorted according to the value they take in the cost function, see e.g. RobustICA [7], FastICA [8]. However, when considering the *a priori* constraint of a narrow spectrum, most algorithms lack the possibility to include this without going to excessive computational complexity, see e.g. the number of tensor slices or correlation matrices needed in JADE [4]-like, respectively SOBI [9]-like, algorithms especially when applied to high data dimensionalities n.

Givens Rotations. The method proposed here is an extraction (or deflation) approach with pairwise optimisation. The advantage is that there exists an algebraic expression able to update the source estimates, avoiding computationally

unattractive search methods. Moreover, since the signals are prewhitened (i.e. mutually decorrelated), it suffices to find an orthogonal matrix to find maximally independent source estimates. We can thus constrain our parameter space to only one parameter per signal pair if we do not take into account permutation and scaling, which are irrelevant parameters when considering the independence criterion. Our search space can thus be limited to the optimal rotation angle for each pair to process [4,3]. This amounts to the following algorithm for prewhitened signals $\hat{\boldsymbol{z}} \in \mathbb{R}^{n\times 1}$:

$$\hat{\boldsymbol{x}}_{ij} = \boldsymbol{Q}\left(\theta_\star\right)\boldsymbol{x}_{ij} \;\;,\;\; \text{where } \boldsymbol{Q}\left(\theta_\star\right) = \begin{pmatrix} \cos\theta_\star & \sin\theta_\star \\ -\sin\theta_\star & \cos\theta_\star \end{pmatrix}, \tag{2}$$

where $\theta_\star$ is the optimal rotation angle that is to be specified, and the matrix $\boldsymbol{Q}\left(\theta_\star\right)$ represents a plane rotation, also known as Givens rotation. $\boldsymbol{x}_{ij}$ and $\hat{\boldsymbol{x}}_{ij}$ are the ith and jth component of $\boldsymbol{x}$, respectively $\hat{\boldsymbol{x}}$. The result of the left multiplication of the data $\hat{\boldsymbol{x}}_{ij}$ by $\boldsymbol{Q}^{-1} = \boldsymbol{Q}^T$ would thus results in the standarized sources $\hat{\boldsymbol{x}}$, with additional constraints imposed by the objective function to which $\theta_\star$ is a solution. If the objective function is chosen well, these sources are maximally independent, an assumption that is believed to hold true for many, if not all, bioelectrical source signals. When the objective function meets the requirements of being maximal if and only if the components are independent, while being blind to possible permutations and scaling, it becomes a contrast function for ICA [3].

Kurtic Difference as a Contrast. We have shown in [10] that the objective function

$$\Psi\left(\boldsymbol{Q}\right) = \sum_{i=1}^{n} \epsilon_i \kappa_{iiii}^{\hat{\boldsymbol{x}}} \tag{3}$$

fulfils all requirements to be a contrast function for ICA, where ϵ_i is the sign of the fourth order auto cumulant of the ith source and $\kappa_{iiii}^{\hat{\boldsymbol{x}}}$ the fourth order cumulant of the ith output. Based on this fact, together with the assumption that the atrial activity caused by AF is a (the sole) platokurtic source in the ECG, the contrast would translate into:

$$\Psi_{AF}\left(\boldsymbol{Q}\right) = \left(\sum_{i=2}^{n} \kappa_{iiii}^{\hat{\boldsymbol{x}}}\right) - \kappa_{1111}^{\hat{\boldsymbol{x}}}, \tag{4}$$

which can be solved using subsequent Givens rotations as defined above. The next paragraph gives the algebraic solution for θ when a pair of signals is considered.

The Optimal θ-value: $\theta_\star$. We can now obtain the optimal value for θ, $\theta_\star$, by calculating the stationary point of our contrast function Ψ_{AF} (4) by setting its derivative to zero. It is sufficient to consider the pairs with opposite kurtosis signs, the other cases being known. As a function of the observed whitened signals $\hat{\boldsymbol{x}} = \boldsymbol{Q}\boldsymbol{x}$ we obtain for Ψ_{AF}:

$$\Psi_{AF}\left(\theta\right) = \lambda_2 - \lambda_1 = \alpha\cos 2\theta + 2\beta\sin 2\theta, \tag{5}$$

where α and β are given by $\left(\kappa_{1111}^{\hat{\boldsymbol{x}}} - \kappa_{2222}^{\hat{\boldsymbol{x}}}\right)$ and $\left(\kappa_{1112}^{\hat{\boldsymbol{x}}} + \kappa_{1222}^{\hat{\boldsymbol{x}}}\right)$, respectively and λ_1, λ_2 are the kurtosis values of $\hat{\boldsymbol{x}}_{ij}$, which can be written as a multi linear function of the source kurtosis values [3] using Eq. (2). Equation 5 has its stationary points at

$$2\theta_\star = \arctan \frac{2\beta}{\alpha}, \tag{6}$$

where $\theta_\star$ is the rotation angle to be found.

Equation 6 is also the equation obtained in [11] based on centroid estimators.

2.2 Inclusion of the Spectral Concentration Constraint

AF is typically characterised by a sinusoidal to triangular waveform (depending on the relative power in the harmonics) with a frequency and amplitude modulation. This spectrally rather narrow banded signal has its main frequency in the 3 to 12 Hz band. This enables us to create additional constraints regarding the spectra, forcing us to redefine the update sequence of the pairwise processing for source extraction as given in [10]. The method extends the natural sweeping procedure for source extraction to a criterion based sweeping procedure. The update criterion is given as

Criterion 1. *Replace the source estimates $\hat{x}_i$ and $\hat{x}_j$ with their updates $\hat{x}_i^\star$ and $\hat{x}_j^\star$ by using the relation $\hat{\boldsymbol{x}}_{ij}^\star = \boldsymbol{Q}^T \hat{\boldsymbol{x}}_{ij}$ iff the spectral concentration in the 3-12Hz band of one of the new estimates exceeds the spectral concentration of the reference source estimate.*

The spectral concentration in criterion 1 is taken as the ratio of spectral density in a $\pm 10\%$ band around the center frequency f_c to the total energy in the signal's spectrum, i.e. $SC = \int_{.9f_c}^{1.1f_c} P(\tau)\mathrm{e}^{-2\pi\tau f}\mathrm{d}f \Big/ \int_{0}^{Fs/2} P(\tau)\mathrm{e}^{-2\pi\tau f}\mathrm{d}f$, if $f_c \in [3\mathrm{Hz}, 12\mathrm{Hz}]$, otherwise $SC = 0$. With this information we can define the sweep procedure as described in table 1, where the stopping criterion is defined to be positive when a sweep occurs without update of the reference source estimate.

Table 1. The pseudo-code for the sweep algorithm

Initialise reference source with $\hat{\boldsymbol{x}}_1$
While false(stopping criterion)
StartSweep: For j from 2 to m
Compute $\theta_\star$ for the reference source estimate $\hat{\boldsymbol{x}}_1$ and estimate $\hat{\boldsymbol{x}}_j$
Compute spectral concentration for $\hat{\boldsymbol{x}}_1^\star$ and $\hat{\boldsymbol{x}}_j^\star$
If criterion 1: replace $\hat{\boldsymbol{x}}_1$ ($\hat{\boldsymbol{x}}_j$) with $\hat{\boldsymbol{x}}^\star$ having highest (lowest) SC
EndSweep

3 Results

3.1 Data

Patient Data. The data upon which the algorithm was run consists of 51 patient registrations with known AF. All ECG sets are standard 12 lead ECG measurements consisting of the leads I-III, aVR, aVL, aLL and the potentials at the electrodes V1-V6. The dataset is by definition overdetermined for the biopotentials since I-III, aVR, aVL and aLL can all be expressed in terms of the left arm (LA), right arm (RA) and left leg (LL) electrode potentials. This means that there is a redundancy of factor 2 in the leads. If we take the LL electrode as the reference electrode for all measurements (which is generally the physical measurement setup), then we are left with 8 independent variables. We can thus reduce our set to 8 recording sites or derivations only without compromising the information in the data. Taking V1-V6 and extracting the potentials at LA and RA from the leads would eliminate this data redundancy.

One has to be careful though in highly noisy environments where the noise at the electrodes is not stationary and the noise term would thus take a sufficiently high amount of the total data subspace. In that case it might not suffice to take only the 8 electrode potentials and the extra derivations might add extra information to solve the ill-conditioned problem.

Simulated Data. To have an idea of the quality of separation we introduce a simulated dataset. This dataset contains an AF signal constructed following the method in [12], whereas the QRS-T simulation has been done using high kurtosis components using the model:

$$\text{QRS-T}_i(t) = \sum_j \tan\left(a_j(t) \sin\left(j\omega(t)\, t\right)\right). \tag{7}$$

The model allows for amplitude modulation in a_j, where $\max_t \sum_j |a_j(t)| \leq 1$, and modulation in $\omega(t)$. By changing the number of harmonics and the parameters in the modulations we can change the statistics of the total time series. Additionally we added two sources that are of no physiological meaning but have a positive kurtosis value, so we do not violate the model assumptions. The randomly drawn square mixing matrix is orthonormal, avoiding the need of the prior whitening step as described in the introduction without restricting the generality.

3.2 Estimating the Central Frequency

To evaluate our method, we focus on the value of the main frequency estimated by our method. The main frequency is defined as the frequency at which the power spectral density is the highest in the 3 - 12Hz band. For the 51 patient registrations we compare the resulting frequencies with those found from a combined FastICA and SOBI approach as it was applied in [13]. We compare the

results as well for AEML, EML and the combEML methods [11] in the same constrained updating framework. In table 2 the results of the central frequency difference among the methods with their respective standard deviation are displayed. To exclude biasing toward short time artefactual instances in the data, the data has been resampled at each iteration before calculation of the optimal rotation angle $\theta_\star$ based on a bootstrap sampling, allowing for overlap. We choose a bootstrap sample size of $2 \cdot 10^3$. To exclude the bootstrap based differences between the methods, we consider 100 Monte Carlo runs per method over the whole dataset of which the mean of the results so obtained are used as the frequencies to construct table 2.

Table 2. Differences in main frequency estimation. The upper right triangle displays the results when 12 leads are considered, in the lower left triangle displays the results for the reduced set of 8 electrode potentials are given.

	fastICA+SOBI	AEMLa	AEMLc	combEML
fastICA+SOBI	0	-0.026 (0.444)	0.083 (0.294)	0.425 (0.429)
AEMLa	0.467 (1.025)	0	0.142 (0.384)	0.032 (0.291)
AEMLc	0.291 (0.526)	-0.085 (0.755)	0	-0.110 (0.338)
combEML	0.425 (0.761)	0.063 (0.767)	0.148 (0.390)	0

Visualisation of the Results. To evaluate the performance on simulated and real datasets, we present the artificial mixture, respectively the observations of the electrode potentials and the source extraction results in Figs. (1) & (2).

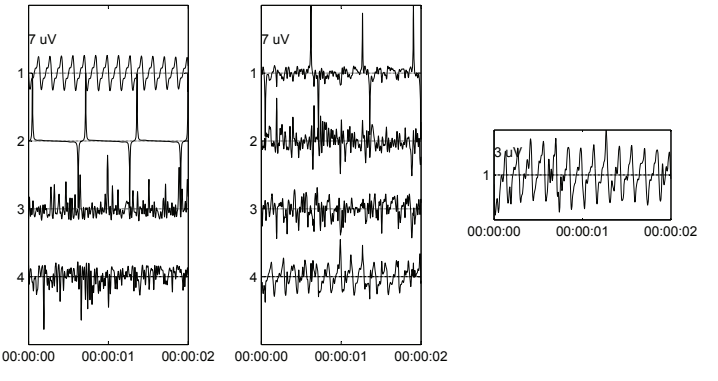

Fig. 1. Extraction of an AF like signal from an artificially generated mixture. left: the original sources; center: the mixture; right: the extracted source.

Fig. (3) gives the PSD for both source estimates in Figs. (1) & (2).

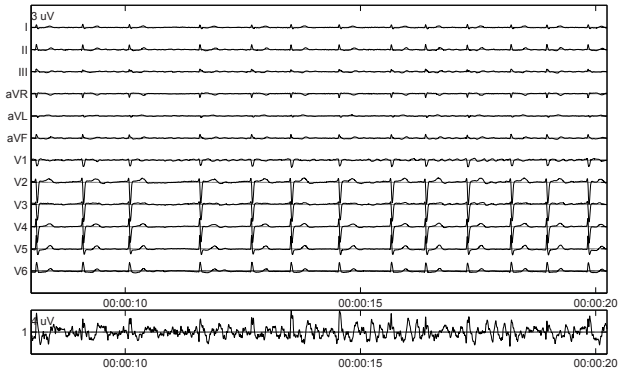

Fig. 2. Extraction of an AF signal from the ECG. upper: 12 channel ECG signal; lower: extracted AF signal.

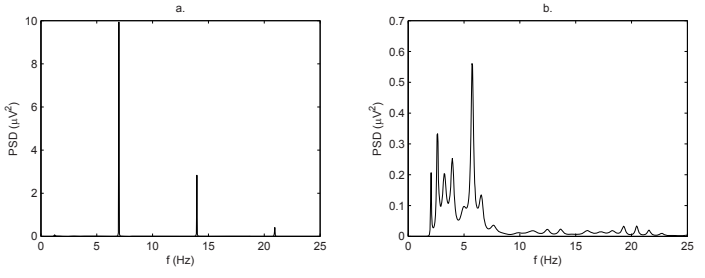

Fig. 3. PSD for the extracted sources from (a) the artificially generated mixture in Fig. (1) and (b) the ECG signal in Fig. (2)

4 Discussion

From Table 2 it is clear that From the figures we can see that the restriction of the spectral concentration does not prevent to extract signals with multiple harmonics, a result that is supported by the fact that the main harmonic is still the central frequency. Moreover, the sources are maximally independent, being a solution to the contrast in [10] subjected to the constraint of spectral concentration in the 3-12Hz band. Moreover, since our technique is based on source extraction, there is no need to do a full decomposition with *a posteriori* source selection, which is computationally attractive, since the overall complexity is of order $\mathcal{O}$ (7n-7)T.

5 Conclusion

The results of the method based on constrained extended AEML are promising toward the extraction of AF from the ECG. Although the presented values and

figures are already showing the strengths of the method, it remains to explore how to obtain a quantitative and objective measure for the evaluation of the proposed source extraction technique against the widely accepted techniques of unmasking the AF through suppression of the QRS-T complex.

References

1. Castells, F., Igual, J., Millet, J., Rieta, J.: Atrial activity extraction from atrial fibrillation episodes based on maximum likelihood source separation. Signal Processing 85, 523–535 (2005)
2. Comon, P.: Analyse en composantes indépendantes et identification aveugle. Traitement du signal 7(3), 435–450 (1990) (Numero special non lineaire et non gaussien)
3. Comon, P.: Independent component analysis, a new concept? Signal Processing 36, 287–314 (1994)
4. Cardoso, J.F.: High-order contrasts for independent component analysis. Neural Computation 11, 157–192 (1999)
5. Lee, T.W., Girolami, M., Bell, A.J., Sejnowski, T.J.: A unifying information-theoretic framework for independent component analysis. International Journal on Mathematical and Computer Modeling (1998)
6. Delfosse, N., Loubaton, P.: Adaptive separation of independent sources: a deflation approach. In: IEEE International Conference on Acoustics, Speech, and Signal Processing (ICASSP'94), Adelaide, Australia, 19-22 April 1994, vol. 4, pp. 41–44. IEEE Computer Society Press, Los Alamitos (1994)
7. Zarzoso, V., Comon, P.: How fast is FastICA? In: Proceedings of the 14th European Signal Processing Conference (EUSIPCO), Firenze, Italy (September 2006)
8. Hyvärinen, A., Oja, E.: A fast fixed-point algorithm for independent component analysis. Neur. Comp. 9, 1483–1492 (1997)
9. Belouchrani, A., Abed-meraim, K., Cardoso, J., Moulines, E.: A blind source separation technique using second order statistics. IEEE Trans on Sign. Proc. 45(2), 434–444 (1997)
10. Phlypo, R., Zarzoso, V., Comon, P., D'Asseler, Y., Lemahieu, I.: ISRN I3S/RR-2007-13-FR: A contrast for ICA based on the knowledge of source kurtosis signs. Technical report, I3S, Sophia Antipolis, France (2007), `http://www.i3s.unice.fr/~mh/RR/2007/liste-2007.html`
11. Zarzoso, V., Nandi, A.K., Hermann, F., Millet-Roig, J.: Combined estimation scheme for blind source separation with arbitrary source PDFs. IEE Electronics Letters 37(2), 132–133 (2001)
12. Stridh, M., Sörnmo, L.: Spatiotemporal qrst cancellation techniques for analysis of atrial fibrillation. IEEE Trans. Biomed. Eng. 48(1), 105–111 (2001)
13. Castells, F., Rieta, J., Millet, J., Zarzoso, V.: Spatiotemporal blind source separation approach to atrial activity estimation in atrial tachyarrhythmias. Biomedical Engineering, IEEE Transactions on 52(2), 258–267 (2005)